

COMPUTER-AIDED DIAGNOSIS OF ALZHEIMER'S DISEASE USING T-SUM FEATURE OBTAINED FROM BRAIN ¹⁸F-FDG PET IMAGE UTILISING SUPPORT VECTOR MACHINE

Said Mahdi Mutahari^{1,2}, Tawatchai Ekjeen^{1,*}, Yudthaphon Vichianin¹,
Khajonsak Tantiwetchayanon¹, and Alzheimer's Disease Neuroimaging Initiative[†]

¹Department of Radiological Technology, Faculty of Medical Technology, Mahidol University, Bangkok, Thailand

²Department of Radiology, Faculty of Allied Health, Kabul University of Medical Sciences, Kabul, Afghanistan

ABSTRACT

T-sum score is a well-known value representing the deviation of metabolism in the brain due to neurodegenerative disease. The score can be obtained from voxel-based statistical analysis of ¹⁸F-FDG PET images. The objective of this study was to explore the enhanced potency of t-sum score for classification of Alzheimer's disease (AD) using support vector machine (SVM). ¹⁸F-FDG PET studies from 100 AD patients and 100 age-matched normal-elderly controls obtained retrospectively from the online ADNI database. Five pre-processing tasks including converting the file format, re-orientation, spatial normalisation, smoothing and intensity normalisation were applied on each PET image. Then, AD t-sum scores were calculated for each subject's PET study through voxel-based analyses using statistical parametric mapping (SPM12) software. The SVM was then employed and the hyperparameters have been optimised through GridSearch technique for computer-aided detection of AD based on AD t-sum feature. The classification accuracy, sensitivity, specificity and AUC based on 10-fold cross-validation were 86%, 84%, 88% and 0.916, respectively. This study showed that employing SVM with optimised hyperparameters based on AD t-sum feature extracted from brain ¹⁸F-FDG PET images provides a good performance for classification of AD.

Keywords: Alzheimer's disease, ¹⁸F-FDG PET, t-sum score, support vector machine, ADNI

Manuscript received on April 13, 2020; revised on June 22, 2020.

^{1,*}Corresponding author E mail: tawatchai.ekj@mahidol.edu
Department of Radiological Technology, Faculty of Medical Technology, Mahidol University, Thailand.

1. INTRODUCTION

Alzheimer's disease (AD), the 6th cause of death worldwide, is a progressive and non-reversible neurodegenerative disorder characterised by impairment in memory and cognition, and followed by alteration in behavior and increasing needs for care [1, 2]. One in 10 people (10%) in the age of 65 years or older has AD in the US in 2020 [3]. Based on an estimation from the World Health Organization (WHO), in 2019 around 30-35 million people across the world suffered from AD [4], and one out of 85 persons will have the AD by 2050 [5]. The typical pathophysiology of AD includes abnormal accumulation of Amyloid beta peptides between neurons forming amyloid plaques that block neural connection, and hyperphosphorylation of tau proteins inside neurons building up neurofibrillary tangles that cause loss of axonal transport [6, 7]. These series of events result in some morphological, metabolic and biochemical changes in the brain happening even before the disease symptoms appear [8].

The morphological changes due to AD including atrophy in the temporal lobe, volume reduction especially in hippocampus and brain ventricles enlargement, can be detected in structural MRI [6]. However, metabolic changes as a predictor of the disease can be detected in the early stages compared to structural alterations [9]. Positron emission tomography (PET) utilizing [¹⁸F]-fluorodeoxyglucose (¹⁸F-FDG) represents the metabolic rate of glucose consumption in vivo. The typical pattern of AD in ¹⁸F-FDG PET images includes hypometabolism in precuneus, bilateral temporo-parietal and frontal cortex, and posterior cingulate area, while primary cortical regions, cerebellum, brainstem, basal ganglia and thalamus are preserved from AD [10, 11].

Through visual assessment of the brain ¹⁸F-FDG PET images by radiologists, subtle metabolic changes in the early AD stages make it difficult to distinguish AD from normal-aging. It causes inter-observer errors when visual assessment of PET data for detection of abnormalities [11]. Over recent years, in order to enhance the radiologists' performance and for reducing inter-observer errors, several computer-aided diagnosis (CAD) procedures for detection

[†]Data used in preparation of this article were obtained from the Alzheimer's Disease Neuroimaging Initiative (ADNI) database (adni.loni.usc.edu). As such, the investigators within the ADNI contributed to the design and implementation of ADNI and/or provided data but did not participate in analysis or writing of this report. A complete listing of ADNI investigators can be found at: http://adni.loni.usc.edu/wp-content/uploads/how_to_apply/ADNI_Acknowledgement_List.pdf

of those metabolic changes have been developed. As a result, radiologists benefit from the diagnosis made by computers as “second opinion” [12-14].

Voxel-based analysis approaches for CAD of AD using ^{18}F -FDG PET images have been the focus of attention of many studies in recent years. In voxel-as-feature (VAF) approach, each individual voxel is considered as a feature. Despite providing a good classification performance, the feature space would be very high dimensional, and causes a very high computational cost [13, 15, 16]. Projection-based approaches also use whole voxels in the image as features, and reduce the number of features using techniques like principal component analysis (PCA), but the feature space would be still high dimensional [17]. Atlas-based approaches map PET images into atlases parcellated into some predefined areas, and each feature would be the summation of voxel values in each region. Despite providing good results, this method needs co-registered MRI from patients to map PET images into atlases [18].

A voxel-based t-test analysis method for CAD of AD was proposed by Perani et al. [19], that calculated t-values for each individual voxel position between each subject's ^{18}F -FDG PET image versus group of age-matched normal controls' images of ^{18}F -FDG PET. Next, an AD mask was created through voxel-based statistical analysis between images from group of AD patients versus group of age-matched control. This mask represented areas that were affected by AD. Lastly, summation of t-values in areas affected by AD in this AD mask provided “t-sum score”. Haense et al. used this score for detection of AD from brain ^{18}F -FDG PET data. they set a pre-defined cut-off value on t-sum score. A subject with t-sum value above that cut-off value was considered as an AD patient and under that value was classified as normal subject. They reported a sensitivity of 83% and specificity of 78% using PET data obtained from ADNI database [11]. This research group also developed a software to detect AD based on this score [20]. A study by Lange and his co-investigators reported an AUC value of 0.832 for detection of AD based on t-sum score [21].

An important component of any CAD system is the classification algorithm that mainly works based on machine learning (ML) principles. Machine learning as a subset of Artificial Intelligence (AI) enables computer systems to be learned from a sampled data set and then, to make a prediction for unseen data [22]. Support vector machine (SVM) is one of the most efficient ML algorithms for the classification task, especially when a small training dataset is available [23]. A meta-analysis on utilization of ML algorithms in healthcare showed that SVM has been the most commonly used classification algorithms in healthcare, especially in the field of neuroimaging [24]. Several studies for computer-aided diagnosis of AD using brain ^{18}F -FDG PET images have used SVM algorithm for the classification task [16, 18, 25-27]. Buchpiguel et al. reported an AUC value of ~ 0.8 for CAD of AD using brain ^{18}F -FDG PET data by employing SVM [28]. Hinrichs et al.

obtained an accuracy of 84% for detection of AD using SVM [25]. SVM was firstly proposed by Cortes and Vapnik [23]. This algorithm attempts to find an optimum hyper-plane for separating data points linearly. If datapoints are not linearly separable, SVM can map datapoints into a new higher dimensional space using various kernel functions like polynomial functions (poly-kernels) and gaussian function (radial-basis function (RBF) kernel) to make datapoint linearly separable [22, 23]. A study by Romero et al. compared the accuracies gained by linear, RBF, polynomial and quadratic SVM kernels for computer-aided diagnosis of AD using brain SPECT images, and showed that RBF kernel yielded the highest classification performance [29]. According to Jongkreangkrai et al. recommendation, the RBF kernel is better to start with while using SVM models [30]. To find the optimised hyperparameters of SVM models, a GridSearch method systematically combines different values of hyperparameters and seeks for the best combination based on the least classification error [31].

Since AD t-sum score is considered as an indicator for detection of AD from brain ^{18}F -FDG PET images, the current study aimed at enhancing the potency of this score for computer-aided diagnosis of AD. To do that, some pre-processing tasks in the process of obtaining AD t-sum score were modified. Then, an SVM with RBF kernel was employed and its hyperparameters were optimised using GridSearch technique. In addition, the area under the ROC curve (AUC) value based on 10-fold cross-validation was used to evaluate the classification performance of the model.

2. MATERIALS AND METHODS

2.1. Data Collection

Brain ^{18}F -FDG PET data used in this study were collected retrospectively from the Alzheimer's Disease Neuroimaging Initiative (ADNI) database (<http://adni.loni.usc.edu>). The ADNI was launched in 2003 as a public-private partnership led by Principal Investigator Michael W. Weiner, MD. The primary goal of ADNI is to test whether serial MRI, PET, other biological markers, clinical and neuropsychological assessment can be combined to measure the progression of MCI and early AD.

A total of 200 studies of the brain ^{18}F -FDG PET were included in this work: 100 from patients with AD (50 men and 50 women; 74 ± 5 years of age; mean age, 73.7; SD: 2.6) and 100 from age-matched normal-elderly subjects (51 men and 49 women; 74 ± 5 years of age; mean age: 74.0; SD: 2.7). The ADNI protocol for ^{18}F -FDG PET data acquisition was: injection of ^{18}F -FDG with activity of 185 MBq (5.0 mCi) ± 10 , 30 minutes (six 5-minutes frames) dynamic acquisition starting from 30 to 60 minutes post-injection.

2.2. Pre-processing

The aim of pre-processing tasks was to make PET images obtained from different systems similar before performing feature extraction. This step has a crucial role in voxel-based statistical analysis which is the basis of current work for extraction of t-sum feature from each image. All five pre-processing tasks including converting the file format, re-orientation, spatial normalisation, smoothing, and intensity normalisation were performed using Statistical Parametric Mapping (SPM12) software running in MATLAB version R2018a.

Firstly, PET images in DICOM format were converted into NIFTI, which is a single 3-dimensional neuroimaging file format. Next, through re-orientation task, images were aligned with the brain PET standard space defined by SPM12. Then, spatial normalisation was applied to PET images. This step ensured that each voxel would refer to the same anatomical region in the brain in all subjects' PET images. A dementia-specific ^{18}F -FDG PET template provided by Caroli et al. [32] was used to register with each subject's PET image. Moreover, smoothing task with the aim of increasing the signal-to-noise ratio and making images more uniform, was applied to images using an isotropic 3-dimensional Gaussian filter with 12 mm full width at half maximum (FWHM).

Since the collected data were with different range of voxels intensities, intensity normalisation was applied as the last pre-processing task. This process was performed according to the method proposed by Fellgiebel et al. [33]. To perform intensity normalisation, a statistical parametric mapping (SPM) process was performed. Statistical parametric mapping refers to an automated voxel-wise statistical comparison of metabolic and functional neuroimages to a group of control. This process is mainly used for identification of those areas in the brain which experience a particular effect such as hypometabolism, hypermetabolism or activation caused by disorders [34, 35]. SPM12 is a software that especially designed to automate this voxel-by-voxel statistical process, and can be used to find those voxel positions either affected or preserved from a specific disease in the brain. In this study, this statistical parametric mapping technique was used for both intensity normalisation and t-sum score extraction tasks from PET data. To normalise the voxel intensities of PET images in the current work, a voxel-by-voxel two-sample t-test between group of PET image from patients with AD versus group of PET images from normal-elderly controls was performed. SPM12 t-contrast was set to find those voxel positions which their mean values in group of AD were higher than in the group of control, with 95% confidence interval (CI) (i.e., SPM12 was commanded to find those statistically significant voxel positions preserved from AD). Fig. 1 represents those voxel positions overlaid on structural MRI images. Using MarsBar software (<http://marsbar.sourceforge.net/>), those voxels were

extracted to form a binary NIFTI image of the preserved area from AD (i.e., voxel positions preserved from AD with value of 1, and those not preserved from AD with value of 0). Then, each subject's PET image was multiplied with this binary image; so, only voxel values remained non-zero which were corresponded to positions preserved from AD. The reference value for normalisation then obtained by averaging the voxel values from the non-zero voxels. The final step for intensity normalisation for each subject's PET image was dividing each voxel value by this reference value using MATLAB software.

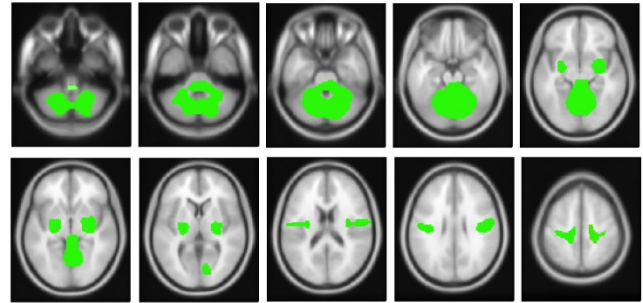


Figure1. Voxel positions preserved from Alzheimer's disease with 95% CI, obtained from voxel-by-voxel statistical analyses, overlaid on structural MRI images.

2.3. AD T-sum Feature Extraction

After all of five pre-processing tasks were accomplished, the whole PET data became similar in term of format, orientation, number of slices, stereotactic voxel position, resolution and range of voxel intensities. In order to extract t-sum feature from each PET study, a three-phased voxel-based statistical process using SPM12 software was performed.

In the first phase, a binary mask of AD was created. To do this, voxel-by-voxel two-sample t-test between group of PET image from patients with AD versus group of PET images from normal-elderly controls was performed in order to find voxel positions which their mean values in group of AD were less than in the group of control, with 95% CI (i.e., statistically significant voxel positions affected by AD). Fig. 2 represents those voxel positions overlaid on structural MRI images. Using MarsBar software, those voxels were extracted to form a binary NIFTI image of the affected area from AD (i.e., voxel positions affected from AD with value of 1, and those not affected by AD with value of 0).

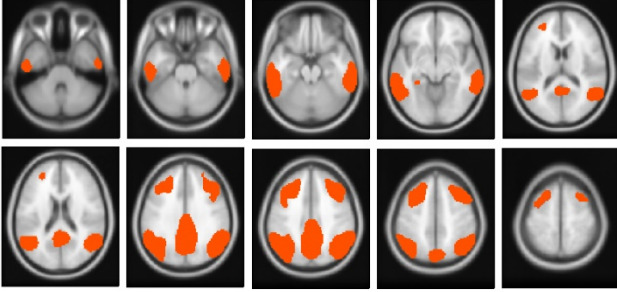


Figure 2. Voxel positions affected from Alzheimer's disease with 95% CI, obtained from voxel-by-voxel statistical analyses, overlaid on structural MRI images.

In the second phase, voxel-by-voxel two-sample t-test between each single subject's PET image versus group of PET images from normal-elderly controls was performed. T-values were then calculated for each voxel position using SPM12, and a 3-dimensional SPM t-map was provided for each individual subject's PET image. This SPM t-map represented how much each subject's PET image differs from group of controls' PET images. However, in this work we only dealt with the differences caused by AD. Hence in the third phase, each subject's SPM t-map was multiplied with the binary mask of AD obtained in the first phase. As a result of this multiplication, only t-values remained non-zero which were corresponded to voxel positions affected from AD. Summation of remaining t-values yielded AD t-sum score, which was the only feature extracted from ^{18}F -FDG PET images in this study.

2.4. Classification Process

The sequential minimal optimization (SMO) algorithm which is an efficient and fast algorithm for training the SVM with RBF kernel was implemented in WEKA data mining suite. WEKA freeware provides ML algorithms in a graphical user interface. A study by Tantiwetchayanon et al. showed that there was no statistically significant difference between the SVM with RBF kernel classification performance implemented in WEKA and SVM-light softwares for computer-aided diagnosis of AD from MRI data [36]. In the current study, WEKA facilitated the cross-validation technique as well as supplying GridSearch option for SVM parameter optimisation.

Classification was performed based on AD t-sum feature extracted from each subject's PET study. Two hyperparameters of RBF kernel, $C = [0^{-6}, 10^{-5}, 10^{-4}, \dots, 10^4, 10^5, 10^6]$ and $\text{Gamma} = [10^{-6}, 10^{-5}, 10^{-4}, \dots, 10^4, 10^5, 10^6]$ were optimised using GridSearch technique. The BuildCalibrationModels option was used for calibrating the fully trained model. Ten-fold cross-validation method was adopted for estimation of classification performance. It means that studies were partitioned into 10 folds (10 small

sets) with equal size where each fold contained 20 PET studies. In the SVM, nine folds were used for training the SVM model and the remaining one fold was used for testing to compute the classification performance. This process was repeated in a loop for 10 times. For the evaluation of the classification performance, sensitivity, specificity and accuracy were computed. Receiver operating characteristic (ROC) analysis was performed using MedCalc statistical software (<https://www.medcalc.org/>). Then, the area under the ROC curve (AUC) was calculated using the same software.

3. RESULTS

Since the greatest risk factor for developing AD is increasing in age [37], to rule out the effect of age from voxel-based analyses, an independent t-test was conducted to compare the age difference between patients with AD and normal-elderly controls. The result showed that there was no significant difference between two groups ($p\text{-value} = 0.37$).

AD t-sum score from each subject's brain ^{18}F -FDG PET image was extracted through statistical parametric mapping. The scatter plot of t-sum features extracted from PET images of AD patients and age-matched controls are illustrated in Fig. 3. It shows scattering of AD t-sum features indicating that using any predefined cut-off value may cause misclassifications. In such situations, machine learning algorithms can find a pattern for the best classification of data points.

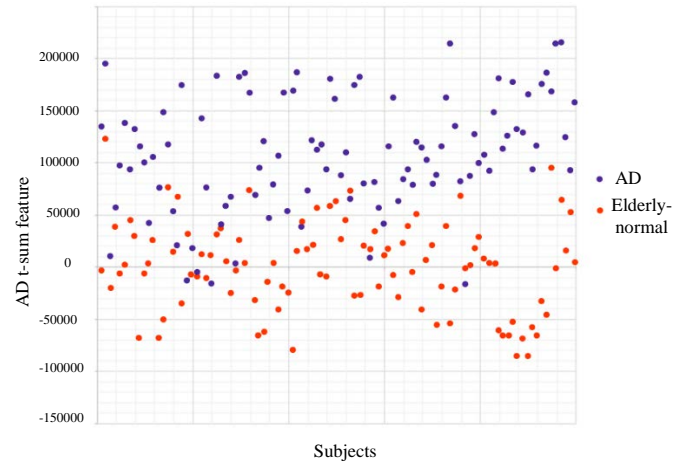


Figure 3. Scatter plot of AD t-sum features extracted from ^{18}F -FDG PET images from 100 patients with AD and 100 normal-elderly controls.

For classification of PET images based on AD t-sum scores in this work, SMO algorithm was employed for training the SVM model, implemented in WEKA data

mining suite. In order to evaluate the enhancement of classification performance of SVM after its hyperparameters optimization through GridSearch technique, ROC for SVM with RBF kernel with the default hyperparameters ($C = 1$ and $\text{Gamma} = 10^{-2}$) defined by WEKA was compared to the SVM with the optimised hyperparameters ($C = 10^6$ and $\text{Gamma} = 10^{-3}$). The obtained AUC values were 0.855 and 0.916, respectively ($P < .001$) (Fig. 4). The sensitivity, specificity, and accuracy after optimization of SVM (with RBF kernel algorithm) hyperparameters were 84%, 88%, and 86%, respectively.

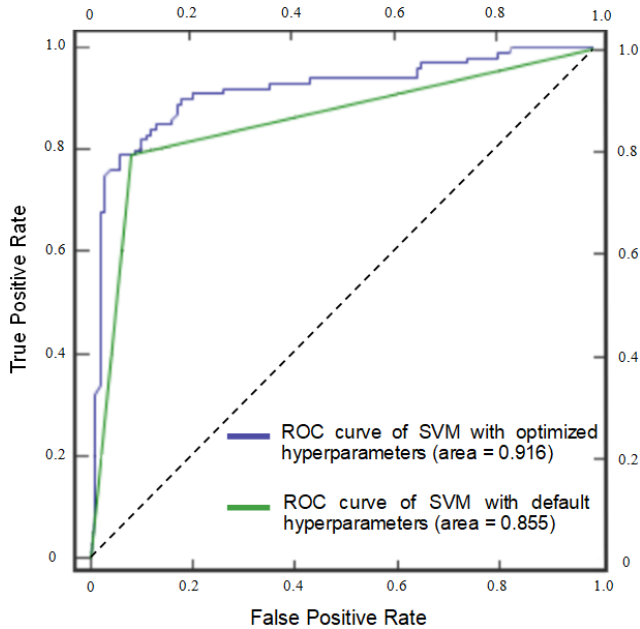


Figure 4. ROC curves and AUC values for evaluation of classification performance of SVMs with optimised and default hyperparameters implemented in WEKA datamining suite.

4. DISCUSSION

Voxel-based statistical analysis approach was the basis of the current study to extract the single value of AD t-sum score from each ^{18}F -FDG PET image. Classification of AD then performed using SVM machine learning algorithm based on AD t-sum score as the only feature element. Utilization of this single feature for building the ML model for classification provided the least computational cost comparing with many studies using voxel-based analysis of PET images for classification of AD. Hinrichs et al. considered each individual voxel of the brain PET images as a feature. As each PET study contains $\sim 5 \times 10^5$ voxels, the high dimensional feature space resulted in a high computation cost for training of the machine

learning algorithm [25]. Andersen et al. reduced the feature space dimensionality by selection of only discriminant voxels between PET data from patients with AD and healthy subjects [16]. However, feature space still remained high dimensions.

T-sum score has been an effective indicator for the deviation of glucose consumption in the brain due to neurodegenerative disorders that can be extracted from brain ^{18}F -FDG PET images. This study tried to modify spatial normalisation, intensity normalisation and smoothing tasks to enhance the potency of this score for detection of Alzheimer's disease. Moreover, instead of using a cut-off value on t-sum score for the classification of PET data, an SVM algorithm was employed and its hyperparameters were optimised to boost the capabilities of t-sum score for computer-aided diagnosis of AD. The proposed method in this study can be useful in clinical researches for the detection of AD from brain ^{18}F FDG PET images.

AD t-sum score firstly proposed by Perani et al [19]. This value represented the deviation of glucose consumption caused by Alzheimer's disease. They performed classification task based on a threshold for t-sum score, obtained sensitivity of 78% and specificity of 83% for classification of AD. Another study by Lange and his co-investigators reported an AUC value of 0.832 for detection of AD based on t-sum score [21]. Fujiwara and his coinvestigators reported a sensitivity of 73% and specificity of 88% using AD t-sum score for estimation of MCI to AD conversion [38]. In current study, we combined voxel-based statistical analysis to obtain AD t-sum score as feature, and SVM was used for classification of AD. Sensitivity of 84%, specificity of 88%, accuracy of 88% and AUC value of 0.916 were obtained for classification of AD.

Intensity normalisation of ^{18}F -FDG PET images prior to voxel-based statistical analysis has an important impact on t-sum feature extraction [21]. Global mean normalisation as the most widely used method in PET analyses, uses the mean value of whole voxels of the brain for intensity normalization. However, this method may provide a bias due to the lower mean value in PET images from patients with AD [39]. Fellgiebel et al. proposed a voxel-based PET group comparison to obtain only voxel positions that were significantly preserved from AD. Then intensity normalisation was performed based on mean value of the preserved voxels from AD [33]. Gjedde et al. suggested intensity normalisation based on voxels preserved from AD to enhance the voxel-based analysis for detection of AD [39]. Similarly, intensity normalisation in this work was performed based on those preserved voxels from AD. These preserved areas from AD were agreed with the study of Fellgiebel et al. [33]. Moreover, the binary mask of AD that represents voxel positions which are significantly affected by AD (with 95% CI), has an important impact on extraction of AD t-sum feature. In this study, the results indicated that these areas were agreed with the results of Lange et al. [21].

The extracted AD t-sum scores from each PET study in this work (Fig. 3), showed variability and scattering of t-sum scores. Thus, it is difficult to determine an appropriate cut-off value for classification of AD. In such situation, machine learning algorithms find a pattern for best classification of datapoints [23]. This was the rationale behind utilization of SVM for classification of AD.

In this study, a single value of AD t-sum score was extracted from each subject's PET image for detection of AD. Further studies can be conducted to split down brain PET images into several regions, in order to extract regional AD t-sum scores from each region in the brain. Then, classification of PET data can be performed using ML algorithms based on regional AD t-sum scores.

There were some limitations in this study. Firstly, this study involved with a binary classification of ^{18}F -FDG PET images into AD or normal-elderly subjects while MCI was not included in this work. Future studies can be conducted for multi-class classification of AD, MCI and normal aging. Secondly, classification task was performed using only one type of ML algorithm which was SVM (SMO with RBF kernel) since SVM is commonly used ML algorithm in healthcare [24]. Other types of ML classifiers such as neural network or decision tree can be employed to compare the performance of SVM algorithm for classification of AD. Lastly, only one feature which was AD t-sum score was an input into the ML algorithm. Inclusion of more features from MRI, the Mini-Mental State Examination (MMSE) score and CSF examination results may enhance the performance for classification of AD in a future study.

5. CONCLUSION

AD t-sum score extracted from brain ^{18}F -FDG PET image through voxel-based statistical approach is a potential biomarker for detection of AD. In the preprocessing step of this work, re-orientation, spatial normalisation, smoothing and intensity normalisation were applied to obtain more accurate values of AD t-sum score. In the classification task, SVM machine learning algorithm was employed and its hyperparameters were optimised. The results of this work indicated high classification performance with accuracy, sensitivity, specificity and AUC values of 86%, 84%, 88% and 0.916, respectively.

6. ACKNOWLEDGEMENT

Data collection and sharing for this project was funded by the Alzheimer's Disease Neuroimaging Initiative (ADNI) (National Institutes of Health Grant U01 AG024904) and DOD ADNI (Department of Defense award number W81XWH-12-2-0012). ADNI is funded by the National Institute on Aging, the National Institute of Biomedical Imaging and Bioengineering, and through generous contributions from the following: AbbVie, Alzheimer's

Association; Alzheimer's Drug Discovery Foundation; Araclon Biotech; BioClinica, Inc.; Biogen; Bristol-Myers Squibb Company; CereSpir, Inc.; Cogstate; Eisai Inc.; Elan Pharmaceuticals, Inc.; Eli Lilly and Company; EuroImmun; F. Hoffmann-La Roche Ltd and its affiliated company Genentech, Inc.; Fujirebio; GE Healthcare; IXICO Ltd.; Janssen Alzheimer Immunotherapy Research & Development, LLC.; Johnson & Johnson Pharmaceutical Research & Development LLC.; Lumosity; Lundbeck; Merck & Co., Inc.; Meso Scale Diagnostics, LLC.; NeuroRx Research; Neurotrack Technologies; Novartis Pharmaceuticals Corporation; Pfizer Inc.; Piramal Imaging; Servier; Takeda Pharmaceutical Company; and Transition Therapeutics. The Canadian Institutes of Health Research is providing funds to support ADNI clinical sites in Canada. Private sector contributions are facilitated by the Foundation for the National Institutes of Health (www.fnih.org). The grantee organization is the Northern California Institute for Research and Education, and the study is coordinated by the Alzheimer's Therapeutic Research Institute at the University of Southern California. ADNI data are disseminated by the Laboratory for Neuro Imaging at the University of Southern California.

The authors extend their thanks to faculty of Medical Technology, Mahidol University.

The first author would like to thank the HEPD Program by Ministry of Higher Education of Afghanistan for providing scholarship for his MSc program and this resultant work.

The first author also thanks Mr. Luca Presotto for his helpful comments for statistical parametric mapping of PET studies.

LIST OF ABBREVIATIONS

AD: Alzheimer's disease, MCI: Mild Cognitive Impairment, ADNI: Alzheimer's Disease Neuroimaging Initiative, AI: Artificial Intelligence, ML: Machine Learning, CAD: Computer-Aided Diagnosis, SVM: Support Vector Machine, SMO: Sequential Minimal Optimization, RBF: Radial-Basis Function, PET: Positron Emission Tomography, ^{18}F -FDG: [18]Fluorine-fluorodeoxyglucose, MRI: Magnetic Resonance Imaging, VAF: Voxel-as-Feature, PCA: Principle component analysis, SPM: Statistical parametric mapping, CI: Confidence Interval, ROC: Receiver Operating Characteristic, AUC: Area Under the Curve, DICOM: Digital Imaging and Communications in Medicine, NIFTI: Neuroimaging Informatics Technology Initiative, SPM: statistical parametric mapping.

REFERENCES

- [1] E.A. Kramarow, and T. Betzaida, "National Vital

- Statistics Reports,” *National Vital Statistics Reports*. Vol. 68, no. 2, Mar.2019.
- [2] B.K. Zetterberg, “Alzheimer's disease,” *Lancet*, vol. 368, no. 95331, pp. 387, 2006.
- [3] Alzheimer's Association, “2020 Alzheimer's disease facts and figures,” *Alzheimer's and Dementia*; vol.16, no. 3, pp. 391– 460, 2020.
- [4] World Health Organisation, “Dementia”. 2019, [Available from: <https://www.who.int/news-room/fact-sheets/detail/dementia>].
- [5] Alzheimer's Association, “2014 Alzheimer's disease facts and figures,” *Alzheimer's and Dementia*; vol.10, no. 2, pp. 47-92, 2014.
- [6] J.R. Hodges, P.J. Nestor, and P. Scheltens, “Advances in the early detection of Alzheimer's disease,” *Nature medicine*, vol. 10, no. 7, pp. S34-S41, Jul. 2004.
- [7] H. Ismail, and L. Wang, “Alzheimer's Disease: A Review of Recent Developments and the Role of Imaging,” *Journal of Nuclear Medicine*, vol. 60, no. supplement 1, pp. 1114. May. 2019.
- [8] R.L. Buckner, “Memory and executive function in aging and AD: multiple factors that cause decline and reserve factors that compensate,” *Neuron*; vol. 44, no. 1, pp. 195-208, Sep. 2004.
- [9] M. Schöll, A Multi-tracer PET approach to study early-onset familial and sporadic Alzheimer's disease, [Ph.D. thesis], Stockholm, Karolinska Institutet, 2011.
- [10] B. Szelies, J. Kessler, K. Herholz, and W.D. Heiss, “Abnormalities of Energy Metabolism in Alzheimer's Disease Studied with PET,” *Annals of the New York Academy of Sciences*, vol. 640, no. 1, pp. 65-71, Dec. 1991.
- [11] C. Haense, K. Herholz, W-D. Heiss, and W.J. Jagust, “Performance of FDG PET for detection of Alzheimer's disease in two independent multicentre samples (NEST-DD and ADNI),” *Dementia and geriatric cognitive disorders*, vol. 28, no. 3, pp. 259-66, 2009.
- [12] K. Doi, “Computer-aided diagnosis in medical imaging: historical review, current status and future potential,” *Computerized medical imaging and graphics*, vol. 31, no. 4, pp. 198-211, Jun. 2007.
- [13] A. Shacklett, C. Davatzikos, M.A. Iftikhar, M. Habes, and S. Rathore, “A review on neuroimaging-based classification studies and associated feature extraction methods for Alzheimer's disease and its prodromal stages,” *NeuroImage*, vol. 155, pp. 530-48, Jul. 2017.
- [14] P. Boonyaphiphat, P. Phukpattaranont, and S. Limsiroratana, “Computer-Aided System for Microscopic Images: Application to Breast Cancer Nuclei Counting,” *IJABME*, vol. 2, no. 1, pp. 69-74, 2009.
- [15] D. Salas-Gonzalez, F. Segovia, I Álvarez, J. Ramírez, J.M. Górriz, M. López, and R. Chaves, “A comparative study of feature extraction methods for the diagnosis of Alzheimer's disease using the ADNI database,” *Neurocomputing*, vol. 75, no. 1, pp. 64-71. Jan. 2012.
- [16] A. Andersen, A. Ivanou, A. Korner, E. Salmon, N. Nelissen, P. Dupont, R. Vandenberghe, and S. Hasselbalch, “Binary classification of 18F-flutemetamol PET using machine learning: comparison with visual reads and structural MRI,” *NeuroImage*, vol. 64, pp. 517-25, Jan. 2013.
- [17] D. Salas-Gonzalez, I. Alvarez, J. Ramirez, J.M. Górriz, M. López, and P. Padilla, “NMF-SVM based CAD tool applied to functional brain images for the diagnosis of Alzheimer's disease,” *IEEE Transactions on medical imaging*, vol. 31, no. 2, pp. 207-16, Sep. 2011.
- [18] A. Hammers, D. Rueckert, K.R. Gray, P. Aljabar, R. Wolz, and R.A. Heckemann, “Multi-region analysis of longitudinal FDG-PET for the classification of Alzheimer's disease,” *NeuroImage*, vol. 60 no. 1, pp. 221-9, Mar. 2012.
- [19] D. Perani, E. Kalbe, E. Salmon, G. Zündorf, J.C. Baron, K. Herholz, K. Ito, L. Frölich, P. Schönknecht, R. Mielke, and V. Holthoff, “Discrimination between Alzheimer dementia and controls by automated analysis of multicenter FDG PET,” *Neuroimage*, vol. 17, no. 1, pp. 302-16, Sep. 2002.
- [20] PMOD-Technologies-LLC, “Alzheimer's Analysis for FDG PET (PALZ),” 2019, [Available from: <http://doc.pmod.com/PDF/PALZ.pdf>].
- [21] C. Lange, L. Frings, L. Spies, P. Suppa, L. Spies, and W. Brenner, “Optimization of statistical single subject analysis of brain FDG PET for the prognosis of mild cognitive impairment-to-Alzheimer's disease conversion,” *Journal of Alzheimer's Disease*, vol. 49, no. 4, pp. 945-59, Jan. 2016.
- [22] A. Ravi, G. Rebala, and S. Churiwala, “An Introduction to Machine Learning”, *Springer*, 2019.
- [23] C. Cortes, and V. Vapnik, “Support-vector networks,” *Machine learning*, vol. 20, no. 3, pp. 273-97, Sep. 1995.
- [24] F. Jiang, H. Li, H. shen, H. Zhi, Q. Dong, S. Ma, Y. Dong, Y. Jiang, and Y. Wang, “Artificial intelligence in healthcare: past, present and future,” *Stroke and vascular neurology*, vol. 2, no. 4, pp. 230-43, 2017.
- [25] C. Hinrichs, G. Xu, L. Mukherjee, M. K. Chung, S.C. Johnson, and V. Singh, “Spatially augmented LPboosting for AD classification with evaluations on the ADNI dataset,” *Neuroimage*, vol. 48, no. 1, pp. 138-49, Oct. 2009.
- [26] C. Cabral, D.C. Costa, and P. M. Morgado, “Predicting conversion from MCI to AD with FDG-PET brain images at different prodromal stages,” *Computers in biology and medicine*, vol. 58, no. 1, pp. 101-9, Mar. 2015.
- [27] A. Chincarini, A. Drzezga, B. N. Van Berckel, F. De Carli, G. B. Frisoni, J. Öberg, et al., “Volume of interest-based [18F] fluorodeoxyglucose PET discriminates MCI converting to Alzheimer's disease from healthy controls. A European Alzheimer's Disease Consortium (EADC) study,” *NeuroImage: Clinical*, vol. 7, no. 1, pp. 34-42, Jan. 2015.
- [28] C. A. Buchpiguel, C. Bottino, C. Leite, C. R. Ono, J. M. Rondina, J. Smid, et al., “Support vector machine-based classification of neuroimages in Alzheimer's disease: direct comparison of FDG-PET, rCBF-SPECT and MRI data acquired from the same individuals,” *Brazilian Journal of Psychiatry*, vol. 40, no. 2, pp. 181-91, Jun. 2018.

[29] A. Romero, D. Salas-Gonzalez, J. M. Górriz, I. Álvarez, J. Ramírez, M. Gómez-Rfo, and M. López, "Computer-aided diagnosis of Alzheimer's type dementia combining support vector machines and discriminant set of features," *Information Sciences*, vol. 237, no. 10, pp. 59-72, Jul. 2013.

[30] C. Jongkreangkrai, "Computer-aided classification of alzheimer's disease based on support vector machine with combination of cerebral image features in MRI," [Master's thesis], Nakhon Pathom, Mahidol University, 2016.

[31] F. Friedrichs, and C. Igel, "Evolutionary tuning of multiple SVM parameters," *Neurocomputing*, vol. 64, pp. 107-17, Mar. 2005.

[32] A. Caroli, A. Prestia, C. Cerami, D. Perani, F. Gallivanone, G. Frisoni, et al., "A standardized [18 F]-FDG-PET template for spatial normalization in statistical parametric mapping of dementia," *Neuroinformatics*, vol. 12, no. 4, pp. 575-93, Oct. 2014.

[33] A. Fellgiebel, A. Hammers, A. Scheurich, I. Schmidtman, H.G. Buchholz, I. Yakushev, et al., "SPM-based count normalization provides excellent discrimination of mild Alzheimer's disease and amnesic mild cognitive impairment from healthy aging," *Neuroimage*, vol. 44, no. 1, pp. 43-50, Jan 2009.

[34] C. Rowe, "Single-photon emission computed tomography in epilepsy," *Magnetic Resonance in Epilepsy*, pp. 385-94, Jan. 2005.

[35] E. Hermans, "SPM12 Starters' Guide," 2016, [Available from: https://www.ernohermans.com/wp-content/uploads/2016/09/spm12_startersguide.Pdf].

[36] C. Ngamsombat, K. Srungboonmee, K. Tantiwetchayanon, O. Chawalparit, T. Ekjeen, and Y. Vichianin, "Comparison of the WEKA and SVM-light based on support vector machine in classifying Alzheimer's disease using structural features from brain MR imaging," *InJournal of Physics: Conference Series*, vol. 1248, no. 1, pp. 12003, Jan. 2019.

[37] J. Bras and R. Guerreiro, "The age factor in Alzheimer's disease," *Genome medicine*, vol. 7, no. 1, pp. 106, 2015.

[38] K. Fujiwara, K. Ito, T. Kato, and T. Yamada, "Estimation of the conversion of mild cognitive impairment to Alzheimer's disease by AD t-sum method," *Journal of Nuclear Medicine*, vol. 52, no. 1, pp. 1264, May 2011.

[39] A. Gjedde, J. Aanerud, P. Borghammer, "Data-driven intensity normalization of PET group comparison studies is superior to global mean normalization," *Neuroimage*, vol. 46, no. 4, pp. 981-8, Jul. 2009.



Said Mahdi Mutahari received his B.Sc. in Radiology Technology from Tehran University of Medical Science, Iran. In 2018, he studied Master's program in Radiological Technology in Mahidol University, Thailand. Currently, he is a university instructor at Department of Radiology, Kabul University of Medical Sciences, Afghanistan. His research interests are AI in the field of medical imaging, nuclear medicine imaging, and medical image quality assessment.



Tawatchai Ekjeen received B.Sc. and M.Sc. degrees in Radiological Technology from Mahidol University, Thailand in 2006 and 2008, respectively. In 2014, he earned Ph.D. in Medical Technology from Mahidol University. Currently, he is a lecturer at Department of Radiological Technology, Faculty of Medical Technology, Mahidol University. His research interests are nuclear medicine imaging, Monte Carlo simulation in nuclear medicine, and medical image quality assessment.



Yudthaphon Vichianin received his B.Sc. in Radiological Technology from Mahidol University, Thailand and M.S. in Information System from Hawai'i Pacific University, U.S.A. He received Ph.D. in Information and Communication Science from University of Hawai'i, Manoa, U.S.A. His research interests are computer simulation in radiological education, PACS, and software application in RT.



Khajonsak Tantiwetchayanon received B.Sc. and M.Sc. degrees in Radiological Technology from Mahidol University, Thailand in 2016 and 2019, respectively. Currently, he is a Radiological Technologist. His research interests are nuclear medicine imaging, MRI, machine learning, deep learning, and AI in medical imaging.